Inorg. Chem. **2003**, *42*, 8847–8852

Synthesis and Characterization of $Ru_2(DMBA)_4X_2$ (X = CN, N_3, $N(CN)_2$, I): Controlling Structural, Redox, and Magnetic Properties with Axial Ligands

Wei-Zhong Chen and Tong Ren*

Department of Chemistry, University of Miami, Coral Gables, Florida 33124

Received September 18, 2003

Metathesis reactions between $Ru_2(DMBA)_4Cl_2$ (DMBA = *N*,*N*′-dimethylbenzamidinate) and MX (M = Na and K) yielded bis-adduct derivatives $Ru_2(DMBA)_4X_2$ (X = CN (**1**), N_3 (**2**), $N(CN)_2$ (**3**)). Metathesis reactions between $Ru_2(DMBA)_4(NO_3)_2$ and KI resulted in $Ru_2(DMBA)_4I_2$ (**4**). Compound **1** is diamagnetic, while compounds **2**–**4** are paramagnetic ($S = 1$). Both compounds **1** and **2** undergo two reversible one-electron processes, an oxidation and a reduction, while compound **3** features a quasireversible reduction. Single-crystal X-ray diffraction studies revealed that the Ru–Ru bond lengths are 2.4508(9), 2.3166(7), 2.304[1], and 2.328(1) Å for compounds **1**–**4**, respectively. Structural and electrochemical data clearly indicate that the axial ligands impart a significant influence on the electronic structures of diruthenium species.

Introduction

Synthesis and characterization of diruthenium paddlewheel species constitute one of the most active fields of metal−metal bonding chemistry.[1,2] Diruthenium species generally display rich characteristics in redox chemistry, spectroscopy, and magnetism, which are attributed to a manifold of ground-state configurations close in energy.[1,3] Hence, diruthenium species have been employed as the building blocks of both supramolecular magnetic materials[4−16] and molecular wires.[17,18] Among hundreds of known diruthenium compounds with bridging ligands such as carboxylate, diarylformamidinate, anilinopyridinate, and hydroxypyridinate, those of a Ru^{II}-Ru^{III} core appear to be the thermodynamically preferred species, although axial coordination by alkynyl ligands resulted in ample examples of Ru^{III}_2 species.[19−28] Recent work from this laboratory established that the Ru^{III}_2 core is preferred with DMBA (*N*,*N*′-dimethylbenzamidinate) bridging ligand.[29−32] Furthermore, while the parent compound

* To whom correspondence should be addressed. E-mail: tren@miami.edu. Tel.: (305) 284-6617. Fax: (305) 284-1880.

(1) Cotton, F. A.; Walton, R. A. *Multiple Bonds between Metal Atoms*; Oxford University Press: Oxford, U.K., 1993.
(2) Aquino, M. A. S. *Coord. Chem. Rev.* **1998**, *170*, 141.
(3) Cotton, F. A.; Yokochi, A. *Inorg. Chem.* **1997**, *36*, 567.
(4) Cotton, F. A.; Kim, Y.; Ren, T. *Inorg. Chem.* **1992**, *31*, 2723.
(5) Cotton, F. A.; Kim, Y.; Ren, T. *Inorg. Chem.* **1992**, *31*, 2608.
(6) Cotton, F. A.; Kim, Y.; Ren, T. *Polyhedron* **1993**, *12*, 607.
(7) Miyasaka, H.; Campos-Fernández, C. S.; Clérac, R.; Dunbar, K. R. *Angew. Chem., Int. Ed.* **2000**, *39*, 3831.
(8) Miyasaka, H.; Clérac, R.; Campos-Fernández, C. S.; Dunbar, K. R. *Inorg. Chem.* **2001**, *40*, 1663.
(9) Miyasaka, H.; Clérac, R.; Campos-Fernández, C. S.; Dunbar, K. R. *J. Chem. Soc., Dalton Trans.* **2001**, 858.
(10) Handa, M.; Sayama, Y.; Mikuriya, M.; Nukada, R.; Hiromitsu, I.; Kasuga, K. *Chem. Lett.* **1996**, 201.
(11) Handa, M.; Sayama, Y.; Mikuriya, M.; Nukada, R.; Hiromitsu, I.; Kasuga, K. *Bull. Chem. Soc. Jpn.* **1998**, *71*, 119.
(12) Handa, M.; Yoshioka, D.; Sayama, Y.; Shiomi, K.; Mikuriya, M.; Hiromitsu, I.; Kasuga, K. *Chem. Lett.* **1999**, 1033.
(13) Yoshioka, D.; Mikuriya, M.; Handa, M. *Chem. Lett.* **2002**, 1044.
(14) Liao, Y.; Shum, W. W.; Miller, J. S. *J. Am. Chem. Soc.* **2002**, *124*, 9336.
(15) Angaridis, P.; Berry, J. F.; Cotton, F. A.; Murillo, C. A.; Wang, X. *J. Am. Chem. Soc.* **2003**, *125*, 10327.
(16) Wesemann, J. L.; Chisholm, M. H. *Inorg. Chem.* **1997**, *36*, 3258.
(17) Ren, T.; Zou, G.; Alvarez, J. C. *Chem. Commun.* **2000**, 1197.
(18) Xu, G.-L.; Zou, G.; Ni, Y.-H.; DeRosa, M. C.; Crutchley, R. J.; Ren, T. *J. Am. Chem. Soc.* **2003**, *125*, 10057.
(19) Ren, T.; Xu, G.-L. *Comments Inorg. Chem.* **2002**, *23*, 355.
(20) Bear, J. L.; Han, B.; Huang, S. *J. Am. Chem. Soc.* **1993**, *115*, 1175.
(21) Li, Y.; Han, B.; Kadish, K. M.; Bear, J. L. *Inorg. Chem.* **1993**, *32*, 4175.
(22) Bear, J. L.; Han, B.; Huang, S.; Kadish, K. M. *Inorg. Chem.* **1996**, *35*, 3012.
(23) Bear, J. L.; Li, Y.; Han, B.; Caemelbecke, E. V.; Kadish, K. M. *Inorg. Chem.* **1997**, *36*, 5449.
(24) Lin, C.; Ren, T.; Valente, E. J.; Zubkowski, J. D. *J. Chem. Soc., Dalton Trans.* **1998**, 571.
(25) Xu, G.-L.; Ren, T. *Inorg. Chem.* **2001**, *40*, 2925.
(26) Xu, G.-L.; Ren, T. *Organometallics* **2001**, *20*, 2400.
(27) Ren, T. *Organometallics* **2002**, *21*, 732.
(28) Xu, G.-L.; Ren, T. *J. Organomet. Chem.* **2002**, *655*, 239.
(29) Xu, G.-L.; Campana, C.; Ren, T. *Inorg. Chem.* **2002**, *41*, 3521.
(30) Xu, G.-L.; Jablonski, C. G.; Ren, T. *Inorg. Chim. Acta* **2003**, *343*, 387.
(31) Xu, G.-L.; Jablonski, C. G.; Ren, T. *J. Organomet. Chem.* **2003**, *683*, 388.

10.1021/ic035106k CCC: $25.00
Published on Web 11/13/2003

Chart 1. DMBA-Bridged Diruthenium Compounds

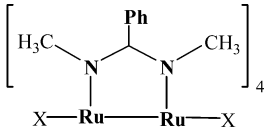

X = CN (**1**); N_3(**2**), $N(CN)_2$ (**3**), I (**4**)

$Ru_2(DMBA)_4Cl_2$ features a short Ru−Ru bond (2.3228(6) Å) and a $S = 1$ ground state, the alkynyl derivatives $Ru_2(DMBA)_4(C_2Y)_2$ (Y = SiR_3, Ph, C_2SiR_3) exhibit both elongated Ru−Ru bonds (ca. 2.45 Å) and a diamagnetic ground state.

In addition to the pursuit of molecular wires based on the $Ru_2(DMBA)_4$ core,[29,31,32] we are also intrigued by its propensity in forming bis-axial adducts $Ru_2(DMBA)_4X_2$. Clearly, this type of compound may function as ditopic ligands with judicious selection of X and serve as a linear linker in a supramolecular construct.[33−35] Reported in this contribution are the syntheses and structural characterizations of a new family of $Ru_2(DMBA)_4X_2$ compounds (Chart 1), where X are potentially bridging ligands CN^- (**1**), N_3^- (**2**), $\{N(CN)_2\}^-$ (**3**), and I^- (**4**).

Results

Compounds **1**−**3** were successfully prepared by reacting $Ru_2(DMBA)_4Cl_2$ with an excess of MX (M = Na or K, X = CN^-, N_3^- and $\{N(CN)_2\}^-$) in satisfactory yields. Although the reaction between $Ru_2(DMBA)_4Cl_2$ and KI did not afford any tractable compound, compound **4** was obtained from the metathesis reaction between $Ru_2(DMBA)_4(NO_3)_2$ and KI. Compounds **1**−**3** are indefinitely stable in ambient atmosphere, while compound **4** decomposes slowly in air.

Compound **1** is diamagnetic and displays well-resolved ^1H and ^{13}C NMR spectra, in agreement with the general observation that cyanide forms exclusively low-spin complexes.[36] Compounds **2**−**4** are paramagnetic with effective magnetic moments of 2.5−3.0 μ_B, which are consistent with a $S = 1$ ground state (theoretical spin-only moment: 2.83 μ_B). The IR spectra of compounds **1**−**3** exhibit stretching bands characteristic of cyanide, azide, and dicyanamide, respectively. The spectrum of compound **1** features a sharp and intense band at 2084 cm^{-1}, which is typical for terminal M−CN complexes.[36] The asymmetric azide stretch in **2** appears as an intense peak at 2030 cm^{-1}. Compared to $\nu(N(CN)_2)$ of the sodium salt of proligand (2287, 2229, 2181 cm^{-1}),[37] those for compound **3** (2263, 2210, 2150) have been red-shifted due to the σ donation to the Ru_2 center upon coordination. Compounds **1**−**3** feature two major peaks in the vis−NIR region of absorption spectra (Figure 1): one at ca. 470 nm and other at ca. 780 nm. Compound **4**, in contrast, displays three well-resolved peaks at 543, 604, and 854 nm, which result in a distinctive blue color.

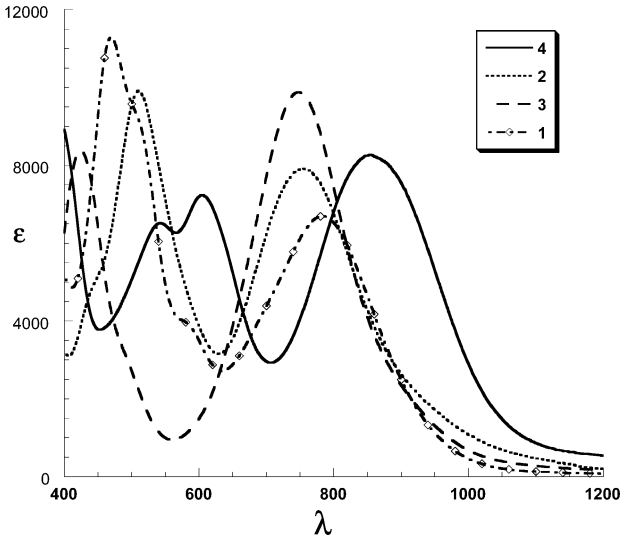

Figure 1. Visible-near infrared (vis−NIR) spectra of compounds **1**−**4** recorded in CH_2Cl_2.

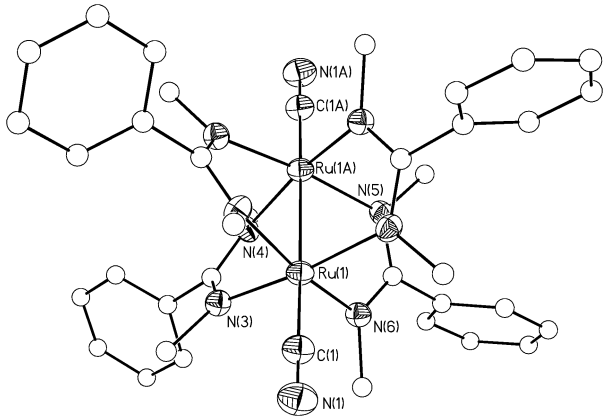

Figure 2. ORTEP plot of molecule **1** at the 30% probability level.

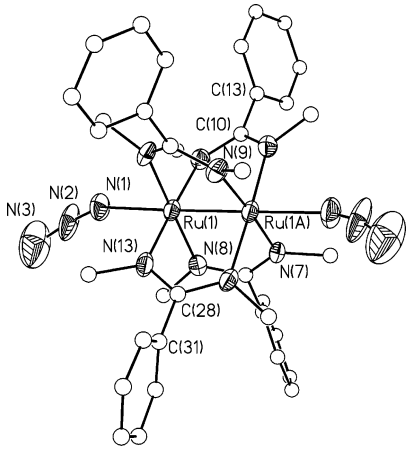

Figure 3. ORTEP plot of molecule **2** at the 30% probability level.

Molecular structures of compounds **1**−**4** were determined through single-crystal X-ray diffraction studies, and the respective structural plots are shown in Figures 2−5. Selected bond lengths and bond angles for compounds **1**−**4** are listed in Table 1. The structural plots clearly illustrate that the overall ligand arrangement around the Ru_2 core in compounds **1**−**4** is very similar to that of the parent molecule $Ru_2(DMBA)_4Cl_2$.[29]

(32) Hurst, S. K.; Xu, G.-L.; Ren, T. *Organometallics* **2003**, *22*, 4118.
(33) Leininger, S.; Olenyuk, B.; Stang, P. J. *Chem. Rev.* **2000**, *100*, 853.
(34) Cotton, F. A.; Lin, C.; Murillo, C. A. *Acc. Chem. Res.* **2001**, *34*, 759.
(35) Cotton, F. A.; Lin, C.; Murillo, C. A. *Proc. Nat. Acad. Sci. U.S.A.* **2002**, *99*, 4810.
(36) Dunbar, K. R.; Heintz, R. A. *Prog. Inorg. Chem.* **1997**, *45*, 283.
(37) Zhang, L.-Y.; Shi, L.-X.; Chen, Z.-N. *Inorg. Chem.* **2003**, *42*, 633.

Table 1. Selected Bond Lengths (Å) and Angles (deg) for Compounds **1**−**4**

1		**2**		**3**		**4**	
Ru1−Ru1′	2.4508(9)	Ru1−Ru1′	2.3166(7)	Ru1−Ru2	2.308(1)	Ru1−Ru2	2.328(1)
Ru1−C1	1.983(5)	Ru1−N1	2.246(4)	Ru1−N1	2.28(1)	Ru1−I1	2.917(1)
Ru1−N3	2.004(4)	Ru1−N7	2.036(5)	Ru2−N4	2.29(1)	Ru2−I2	2.960(1)
Ru1−N6	1.991(4)	Ru1−N8	2.036(5)	Ru1−N7	2.06(1)	Ru1−N1	2.041(6)
Ru1−N4	2.096(4)	Ru1−N9	2.033(4)	Ru1−N9	2.053(9)	Ru2−N2	2.059(6)
Ru1−N5	2.084(4)	Ru1−N13	2.040(3)	Ru1−N12	2.043(9)	Ru1−N3	2.043(7)
C1−N1	1.139(6)	N1−N2	1.036(5)	Ru1−N14	2.077(9)	Ru2−N4	2.055(7)
		N2−N3	1.158(7)	Ru2−N8	2.069(1)	Ru1−N5	2.038(6)
				Ru2−N10	2.05(1)	Ru2−N6	2.049(6)
				Ru2−N11	2.048(9)	Ru1−N7	2.062(7)
				Ru2−N13	2.023(9)	Ru2−N8	2.053(7)
				N1−C1	1.10(1)		
				C1−N2	1.32(1)		
				N2−C2	1.21(1)		
				C2−N3	1.15(1)		
				N4−C3	1.10(2)		
				C3−N5	1.32(2)		
				N5−C4	1.12(2)		
				C4−N6	1.15(2)		
Ru1′−Ru1−C1	166.8(1)	Ru1′−Ru1−N1	178.7(1)	Ru2−Ru1−N1	178.3(3)	Ru1−Ru2−I2	179.32(4)
Ru1−C1−N1	178.0(5)	Ru1−N1−N2	153.6(5)	Ru1−N1−C1	164(1)	Ru2−Ru1−I1	178.28(4)
		N1−N2−N3	166.5(1)	N1−C1−N2	170(2)		
				C1−N2−C2	121(1)		
				N2−C2−N3	176(3)		
				Ru1−Ru2−N4	179.3(4)		
				Ru2−N4−C3	165(1)		
				N4−C3−N5	168(2)		
				C3−N5−C4	132(2)		

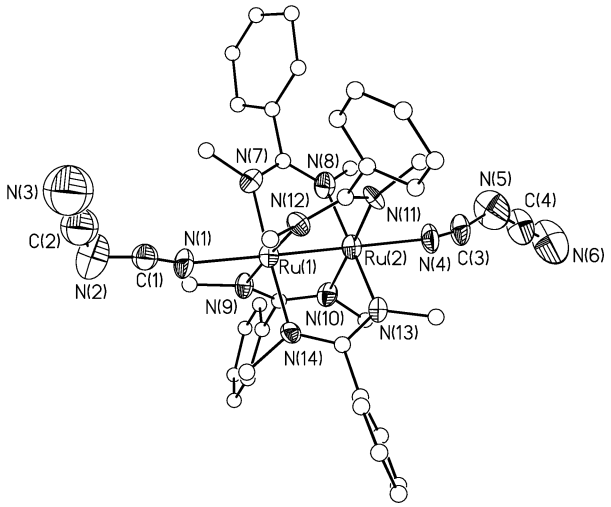

Figure 4. ORTEP plot of molecule **3** at the 30% probability level.

A closer inspection of Table 1 reveals that there are two subsets based on the coordination geometry around the Ru_2 core: molecule **1** and molecules **2**−**4**. The Ru−Ru bond length in **1** is 2.4508(9) Å, which is significantly elongated from that of the parent molecule $Ru_2(DMBA)_4Cl_2$ (2.3224(7) Å) but identical to that of $Ru_2(DMBA)_4(CCTMS)_2$ (2.4501(6) Å).[29] The Ru−C distance in **1** is about 1.983(5) Å, indicating a strong Ru−C σ-bond. Interestingly, two of four crystallographically independent Ru−N bonds (Ru1−N3 and Ru1−N6) are short, while the other two (Ru1−N4 and Ru1−N5) are substantially longer. In addition, the Ru1′−Ru1−C1 angle deviates from linearity by 13°. Such significant structural distortions from an idealized D_{4h} point symmetry were observed previously in other diruthenium(III) species containing either alkynyl or cyano axial ligands[27,38] and attributed to a second-order Jahn−Teller

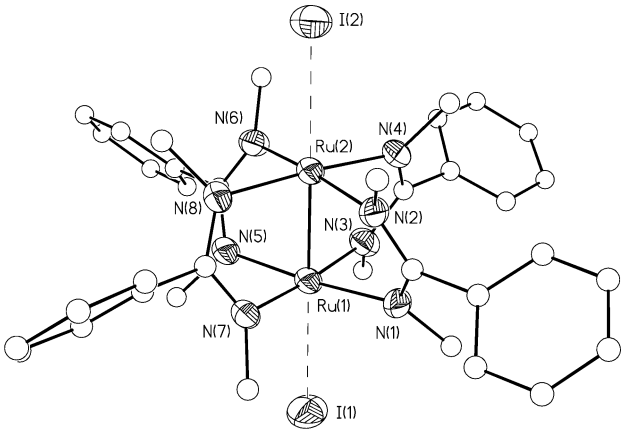

Figure 5. ORTEP plot of molecule **4** at the 30% probability level.

distortion.[24] Structural similarity between **1** and previously studied diruthenium(III) species containing strong donor axial ligands implies that the ground-state configuration of compound **1** is best described as $\pi^4\delta^2\pi^{*4}$ and that **1** contains a Ru−Ru single bond.[3]

In the second subset, Ru−Ru bond lengths found for compounds **2**−**4** are 2.3166(7), 2.3044(14), and 2.3277(10) Å, respectively, and very close to that of $Ru_2(DMBA)_4Cl_2$. In each diruthenium species, the Ru−N bond lengths are within 0.015 Å from the mean value, and the Ru−Ru−L_{ax} angles are very close to 180°. Clearly, the coordination sphere of Ru_2 core in **2**−**4** has an effective D_{4h} symmetry and is not subject to the second-order Jahn−Teller distortion. These structural characteristics as well as the paramagnetism indicate that compounds **2**−**4** have a ground state different

(38) Bear, J. L.; Chen, W.-Z.; Han, B.; Huang, S.; Wang, L.-L.; Thuriere, A.; Caemelbecke, E. V.; Kadish, K. M.; Ren, T. *Inorg. Chem.* **2003**, *42*, 6230.

from that of **1**. Although both $\sigma^2\pi^4\delta^2\pi^{*2}$ and $\pi^4\delta^2\pi^{*2}$ configurations would result in an $S = 1$ state, a relatively short Ru−Ru bond and long Ru−L_{ax} bond in all three cases imply that the former configuration is adopted.

Additional structural details about compounds **2**−**4** worthy of brief discussion are provided below. In molecule **2**, the N(1)−N(2)−N(3) bond angle (166.5(10)°) deviates significantly from linearity, and the N(1)−N(2) bond (1.036(5) Å) is significantly shorter than the N(2)−N(3) bond (1.158(7) Å). These features are associated with both the dative bond from N(1) to Ru(1) and the back-bonding from the diruthenium center to N(1).

The asymmetric unit of crystal **3** contains three independent molecules, among which the metric parameters of the first coordination spheres of Ru_2 core are identical within experimental errors. Hence, metric parameters of one of three molecules were provided in Table 1. Among three compounds containing N-donor axial ligands, molecule **3** has the longest Ru−N_{ax} distances (2.28(1) and 2.29(1) Å), reflecting the weak donor nature of dicyanamide ligand. The N−C distances for the Ru-bound cyano groups (N1−C1, 1.10(1) Å; N4−C3, 1.10 (1) Å) are slightly shorter than that of free cyano groups (C2−N3 = 1.22 (3), C4−N6 = 1.15(2) Å). In comparison, the N−C distances of both Fe-bound and free cyano groups in the structure of $[CpFe(dppe)(N(CN)_2]^+$ were identical within experimental errors.[37]

In molecule **4**, very long Ru−I bond lengths (2.917(1) and 2.960(1) Å) were found from the X-ray diffraction study. They are very close to the sum (2.97 Å) of ionic radii of Ru^{3+} (0.77 Å) and I^- (2.20 Å) and much longer than the sum (2.57 Å) of covalent radii (1.24 and 1.33 Å for Ru and I, respectively).[39] Clearly, the Ru−I bonds in **4** are highly ionic. Axial ligation of iodide is unknown among diruthenium paddlewheel species and generally rare among homodinuclear paddlewheel complexes. Structurally characterized examples include those of Mo^{II}_2,[40] W^{II}_2,[41] Pt^{III}_2,[42−44] and Ir^{II}_2,[45] and the M−I distances are gathered in Table 2. It appears that the M−I bonds are purely ionic with M as early and middle transition metals and become more covalent with M as late transition metals. In a related example, molecular I_2 bridges $Rh_2(O_2CCF_3)_4$ units through strong axial interaction.[46]

As commonly observed for other diruthenium species,[1,19] compounds **1**−**4** display rich features in their cyclic voltammograms shown in Figure 6. Compounds **1** and **2** undergo two reversible one-electron redox processes: one-electron oxidation (**A**) and reduction (**B**) (Scheme 1). It is interesting to note that the $E_{1/2}$(**A**) of **1** is 0.20 V more positive than that of **2**, which is consistent with a significant stabilization of the $\pi^*(Ru_2)$ (HOMO in both **1** and **2**) by the cyano ligand in **1**. On the other hand, the $E_{1/2}$(**B**) of **1** is 0.50 V more negative than that of **2**, which may be attributed to either compounds **1** and **2** having *different* LUMOs or a substantial destabilization of the LUMO in **1** by the CN^- ligand.

In the cases of compounds **3** and **4**, the reduction wave (**B**) is quasireversible or irreversible and immediately followed by a smaller wave (**C**). The latter wave is likely attributed to the reduction of the monoaxially ligated species $Ru_2(DMBA)_4X$ produced by fast dissociation of X^- from $[Ru_2(DMBA)_4X_2]^-$.[29] The oxidation process is unobserved in **3** and irreversible in **4**. Clearly, the Ru−X bond is weak and subject to facile cleavage in both compounds **3** and **4**.

Table 2. M−I Bond Lengths Observed and Comparison with the Sum of Covalent and Ionic Radii[a]

compd	d(M−I), Å	$(r_M + r_I)_{covalent}$, Å	$(r_M + r_I)_{ionic}$, Å
$Ru_2(DMBA)_4I_2$	2.939	2.57	2.97
$Mo_2(dppa)_2(OAc)_2I_2$[b,40]	3.181	2.62	3.12
$W_2(dppm)_2(benzoate)_2I_2$[c,41]	3.103	2.63	3.12
$K_4[Pt_2(P_2O_5H_2)_4I_2]$[42]	2.746	2.62	2.98
$Pt_2(S_2CCH_2Ph)_4I_2$[43]	2.753	2.62	2.98
$Pt_2(2\text{-UT})_4I_2$[d,44]	2.771	2.62	2.98
$[Ir_2(TMB)_4I_2](BPh_4)_2$[e,45]	2.717	2.59	3.09

[a] All radii were taken from ref 39. Ionic radius of W^{2+} is unavailable and estimated to be the same as that of Mo^{2+}. Ionic radius of Pt^{3+} is unavailable and estimated as the mean of Pt^{2+} and Pt^{4+}. [b] dppa = bis(diphenylphosphino)amine. [c] dppm = bis(diphenylphosphino)methane. [d] 2-UT = anion of 2-thiouracil. [e] TMB = 2,5-diisocyano-2,5-dimethylhexane.

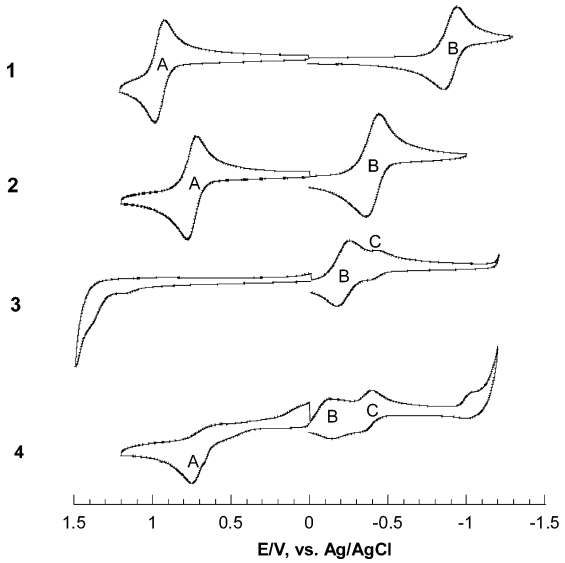

Figure 6. Cyclic voltammograms of compounds **1**−**4** recorded in 0.20 M CH_2Cl_2 solution of Bu_4NPF_6 at a scan rate of 0.10 V/s.

Scheme 1. Electrochemical/Chemical Steps in $Ru_2(DMBA)_4X_2$

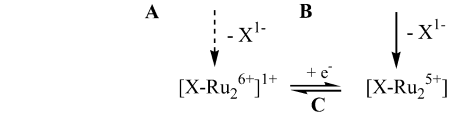

(39) Emsley, J. *The Elements*, 2nd ed.; Oxford: New York, 1991.
(40) Arnold, D. I.; Cotton, F. A.; Kühn, F. E. *Inorg. Chem.* **1996**, *35*, 4733.
(41) Carlson-Day, K. M.; Eglin, J. L.; Lin, C.; Ren, T.; Valente, E. J.; Zubkowski, J. D. *Inorg. Chem.* **1996**, *35*, 4727.
(42) Alexander, K. A.; Bryan, S. A.; Fronczek, F. R.; Fultz, W. C.; Rheingold, A. L.; Roundhill, D. M.; Stein, P.; Watkins, S. F. *Inorg. Chem.* **1985**, *24*, 2803.
(43) Bellitto, C.; Bonamico, M.; Dessy, G.; Fares, V.; Flamini, A. *J. Chem. Soc., Dalton Trans.* **1986**, 595.
(44) Goodgame, D. M. L.; Rollins, R. W.; Slawin, A. M. Z.; Williams, D. J.; Zard, P. W. *Inorg. Chim. Acta* **1986**, *120*, 91.
(45) Maverick, A. W.; Smith, T. P.; Maverick, E. F.; Gray, H. B. *Inorg. Chem.* **1987**, *26*, 4336.
(46) Cotton, F. A.; Dikarev, E. V.; Petrukhina, M. A. *Angew. Chem., Int. Ed.* **2000**, *39*, 2362.

Scheme 2. MO Correlation Diagram between $[Ru2(HNC(H)NH)_4]^{2+}$ and Strong-Field Ligands

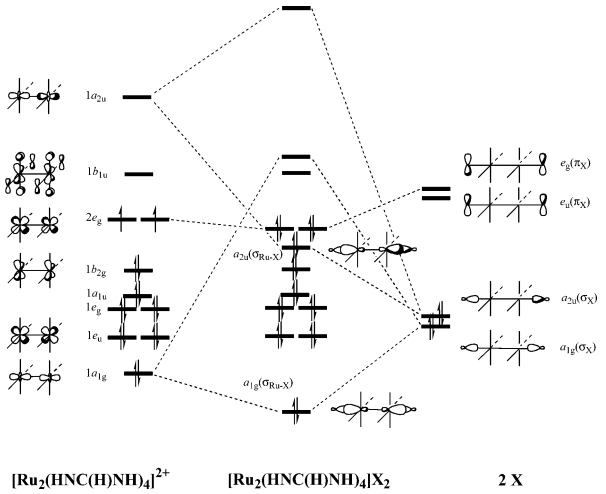

Discussion

The majority of previously reported Ru_2(III) species contains alkynyl[19] and cyano ligands[38] at the axial positions with the exception of $Ru_2(hpp)_4Cl_2$[47] and $Ru_2(DMBA)_4Cl_2$.[29] Combination of the current $Ru_2(DMBA)_4$ series (**1**−**4**) and previously reported alkynyl and chloro compounds provides a unique collection of compounds of the same Ru^{III}_2 core but a variety of axial ligands of different donor strengths. These compounds are clearly divided into two sets: those of alkynyl[29] and cyano (**1**) that are diamagnetic and of long Ru−Ru bond; those of weak field ligands Cl^-, N_3^- (**2**), $N(CN)_2^-$ (**3**), and I^- (**4**) that are paramagnetic and of short Ru−Ru bond. To explain the contrast in electronic properties between two sets, a qualitative MO scheme was constructed on the basis of the SCF−Xα result of $Ru_2(HNC(H)NH)_4$.[48]

SCF−Xα computation of $Ru_2(HNC(H)NH)_4$, a Ru^{II}_2 model compound of $Ru_2(DPhF)_4$, revealed the following valence MOs in ascending energy order: σ(Ru−Ru) ($1a_{1g}$); π(Ru−Ru) ($1e_u$); π(N−C−N) ($1e_g$ and $1a_{1u}$, orbital plots not shown); δ(Ru−Ru) ($1b_{2g}$); π^*(Ru−Ru) ($2e_g$); δ^*(Ru−Ru) ($1b_{1u}$). The order of π^* and δ^* orbitals is inverted from the conventional order of $E(\delta^*) < E(\pi^*)$ because of the destabilization of δ^* by the antibonding contribution from the π_{nb}(N−C−N) orbitals, which results in a ground-state configuration $\sigma^2\pi^4\delta^2\pi^{*4}$ for the Ru^{II}_2 species.[48] On becoming $[Ru_2(HNC(H)NH)_4]^{2+}$, the ground-state configuration should be $\sigma^2\pi^4\delta^2\pi^{*2}$, as shown on the left in Scheme 2. σ-Donor orbitals of weak-field ligands, i.e., Cl^-, N_3^-, $N(CN)_2^-$, and I^-, are both contracted and low-lying in energy and only exert a weak antibonding interaction with σ(Ru−Ru) ($1a_{1g}$) when ligated at the axial positions. Consequently, the overall distribution of Ru_2-based MOs changes little and the $\sigma^2\pi^4\delta^2\pi^{*2}$ configuration is retained for $Ru_2(DMBA)_4X_2$. σ-Donor orbitals of strong field ligands such as CN^- and alkynyl, on the other hand, are close in energy to that of d_σ orbitals of Ru_2 core and more diffused. The bonding interactions between σ_X and d_σ are so strong that the latter on each Ru center is repolarized toward the respective axial ligand. Formation of two σ(Ru−C) bonds implies the demise of σ(Ru−Ru) and results in a singly bonded configuration of $\pi^4\delta^2\pi^{*4}$ that is consistent with the elongation of Ru−Ru bond lengths in both **1** and $Ru_2(DMBA)_4(C_2Y)_2$.[29,31,32] It should be noted that the qualitative model described above does not provide an in-depth answer about either the nature of observed electronic transitions or a quantitative rationale of the observed redox couples. MO calculations on diruthenium compounds at a high level of accuracy, such as ab initio and density functional methods, are needed to address these issues.

Conclusions

In this contribution we have demonstrated that the $Ru_2(DMBA)_4$ core is capable of forming axial adducts of a broad variety of σ-donor ligands, and the resultant compounds can be either diamagnetic or paramagnetic depending on the donor strength of the axial ligands. Compounds bearing ditopic ligands such as CN^-, N_3^-, and $N(CN)_2^-$ may function as ditopic linear linkers themselves, a property that is currently under investigation in our laboratory.

Experimental Section

Potassium cyanide, sodium azide, sodium dicyanamide, and potassium iodide were purchased from ACROS/Fisher Scientific Co., and silica gel was purchased from Merck. $Ru_2(DMBA)_4Cl_2$ and $Ru_2(DMBA)_4(NO_3)_2$ were prepared as previously described.[29,30] ^1H and ^{13}C NMR spectra were recorded on a Bruker AVANCE300 NMR spectrometer, with chemical shifts (δ) referenced to the residual $CHCl_3$ and the solvent $CDCl_3$, respectively. Infrared spectra were recorded on a Perkin-Elmer 2000 FT-IR spectrometer using KBr disks. UV−vis spectra in CH_2Cl_2 were obtained with a Perkin-Elmer Lambda-900 UV−vis spectrophotometer. Magnetic susceptibility was measured at 294 K with a Johnson Matthey Mark-I magnetic susceptibility balance. Elemental analysis was performed by Atlantic Microlab, Norcross, GA. Cyclic voltammograms were recorded in 0.2 M $(n\text{-}Bu)_4NPF_6$ solution (CH_2Cl_2, N_2-degassed) on a CHI620A voltammetric analyzer with a glassy carbon working electrode (diameter = 2 mm), a Pt-wire auxiliary electrode, and a Ag/AgCl reference electrode. The concentration of diruthenium species is always 1.0 mM. The ferrocenium/ferrocene couple was observed at 0.456 V (vs Ag/AgCl) at the experimental conditions.

Preparation of $Ru_2(DMBA)_4(CN)_2$ (1). A round-bottom flask was charged with $Ru_2(DMBA)_4Cl_2$ (200 mg, 0.23 mmol), KCN (61.8 mg, 0.95 mmol), and 40 mL of CH_2Cl_2. After being stirred in air for 2 h, the reaction was terminated. Excess NaCN was removed from the reaction mixture by repetitive water extraction (3 × 20 mL), and the organic phase was dried over Na_2SO_4. Solvent removal resulted in 180 mg of red powder of **1** (93% based on Ru). Data for **1**: R_f (acetone/CH_2Cl_2/hexanes, 1/2/4 v/v/v; the same solvent combination was used for R_f determination thereafter), 0.23; MS-FAB (*m*/*e*, based on ^{101}Ru), 844 [MH^+]. Anal. Found (calcd) for $C_{38}H_{44}N_{10}Ru_2$ (**1**): C, 54.09 (54.14); H, 5.24 (5.26); N, 16.42 (16.62). IR [ν(C≡N)/cm^{-1}]: 2084 (s). UV−vis [λ_{max} (nm, ϵ (M^{-1} cm^{-1})]: 469 (11 300), 783 (6700). ^1H NMR ($CDCl_3$): 7.73−7.42 (m, 12H, aromatic), 7.00−6.93 (m, 8H, aromatic), 3.30 (s, 24H, NCH_3). ^{13}C NMR ($CDCl_3$, C≡N): 134.77. Cyclic voltammogram [$E_{1/2}$/V, ΔE_p/V, $i_{backward}/i_{forward}$]: **A**, 0.944, 0.062, 0.850; **B**, −0.907, 0.086, 0.940.

(47) Bear, J. L.; Li, Y.; Han, B.; Kadish, K. M. *Inorg. Chem.* **1996**, *35*, 1395.
(48) Cotton, F. A.; Ren, T. *Inorg. Chem.* **1991**, *30*, 3675.

Table 3. Crystal Data for Compounds **1**−**4**

	1·2EtOH	**2**	**3**$_3$·EtOAc	**4**
chem formula	$C_{42}H_{44}N_{10}O_2Ru_2$	$C_{36}H_{44}N_{14}Ru_2$	$C_{124}H_{139}N_{42}O_2Ru_6$	$C_{36}H_{44}I_2N_8Ru_2$
fw	923.01	874.99	2856.19	835.79
space group	*C*2/*c* (No. 15)	*Pbcn* (No. 60)	$P\bar{1}$ (No. 2)	$P2_1/n$ (No. 14)
a, Å	18.005(5)	12.255(2)	13.425(3)	12.1989(6)
b, Å	13.995(4)	21.136(3)	20.155(4)	17.3987(9)
c, Å	18.665(6)	15.549(3)	27.587(5)	19.232(1)
α, deg			83.131(4)	
β, deg	104.802(5)		82.778(4)	96.4780(1)
γ, deg			75.228(4)	
V, Å^3	4547(2)	4028(1)	7131(2)	4055.8(4)
Z	4	8	2	4
T, °C	27	27	27	27
λ(Mo Kα), Å	0.710 73	0.710 73	0.710 73	0.710 73
ρ_{calc}, g cm^{-3}	1.366	1.443	1.330	1.711
μ, mm^{-1}	0.709	0.794	0.680	2.302
R	0.046	0.038	0.074	0.055
wR2	0.101	0.097	0.185	0.140

Preparation of $Ru_2(DMBA)_4(N_3)_2$ (2). To a 30 mL THF solution containing 250 mg of $Ru_2(DMBA)_4Cl_2$ (0.29 mmol) was added 94 mg of NaN_3 (1.45 mmol). After being stirred in air for 30 min, the reaction mixture was filtered through a 2 cm silica gel pad. Removal of the solvent from the filtrate yielded 170 mg of red powder (**2**) (67% based on Ru). Data for **2**: R_f, 0.38; MS-FAB (*m*/*e*, based on ^{101}Ru), 823 [$Ru_2(DMBA)_4N_2^+$]. Anal. Found (calcd) for $C_{36}H_{44}N_{14}Ru_2$ (**2**): C, 49.60 (49.42); H, 5.06 (5.07); N, 22.51 (22.41). UV−vis [λ_{max} (nm, ϵ (M^{-1} cm^{-1})]: 509 (9920), 758 (7920). χ_{mol}(corrected) = 3.75 × 10^{-3} emu. μ_{eff} = 2.96 μ_B. Cyclic voltammogram [$E_{1/2}$/V, ΔE_p/V, $i_{backward}/i_{forward}$]: **A**, 0.744, 0.057, 0.876; **B**, −0.418, 0.098, 0.864.

Preparation of $Ru_2(DMBA)_4(N(CN)_2)_2$ (3). This was synthesized using the same procedure as that for **2** and replacing NaN_3 with $NaN(CN)_2$ (129 mg, 1.45 mmol). Compound **3** was isolated as a green microcrystalline material (230 mg, 86%). Data for **3**: R_f, 0.32; MS-FAB (*m*/*e*, based on ^{101}Ru), 926 [M^+H]. Anal. Found (calcd) for $C_{40}H_{44}N_{14}Ru_2$ (**3**): C, 51.89 (52.05); H, 4.80 (4.80); N, 21.18 (21.25). UV−vis [λ_{max} (nm, ϵ (M^{-1} cm^{-1})]: 424 (8380), 748 (9880). χ_{mol}(corrected) = 3.23 × 10^{-3} emu. μ_{eff} = 2.75 μ_B. Cyclic voltammogram [$E_{1/2}$/V, ΔE_p/V, $i_{backward}/i_{forward}$]: **B**, −0.208, 0.069, 0.706.

Preparation of $Ru_2(DMBA)_4I_2$ (4). A round-bottom flask was charged with $Ru_2(DMBA)_4(NO_3)_2$ (200 mg, 0.22 mmol), KI (144 mg, 0.88 mmol), and 40 mL of THF. After being stirred under argon for 1 h, the mixture was filtered through a 2 cm Celite pad. After the removal of THF, the residue was washed with large amount of hexanes and dried under vacuum to yield 160 mg of dark blue compound (70%). Data for **4**: R_f, 0.32; MS-FAB (*m*/*e*, based on ^{101}Ru), 917 [$(M - I)^+$]. Anal. Found (calcd) for $C_{36}H_{50}I_2N_8O_3Ru_2$ (**4**·3H_2O): C, 39.48 (39.35); H, 4.17 (4.59); N, 9.92 (10.20). UV−vis [λ_{max} (nm, ϵ (M^{-1} cm^{-1})]: 543 (6520), 604 (7230), 854 (8280). χ_{mol}(corrected) = 2.57 × 10^{-3} emu. μ_{eff} = 2.45 μ_B. Cyclic voltammogram: E_{pa}(**A**), 0.75 V; E_{pc}(**B**), −0.14 V; E_{pc}(**C**), −0.40 V.

X-ray Data Collection, Processing, and Structure Analysis And Refinement. Single crystals were grown via slow evaporation of either an ethanol solution (**1** and **2**), an ethyl acetate/hexanes solution (**3**), or a CH_2Cl_2/hexanes solution (**4**). The X-ray intensity data were measured at 300 K on a Bruker SMART1000 CCD-based X-ray diffractometer system using Mo Kα (λ = 0.710 73 Å) (Table 3). Thin plates of dimension 0.23 × 0.25 × 0.08 mm^3 (**1**), 0.47 × 0.36 × 0.06 mm^3 (**2**), 0.33 × 0.30 × 0.05 mm^3 (**3**), and 0.35 × 0.11 × 0.03 mm^3 (**4**) were used for X-ray crystallographic analysis. Crystals **1** and **3** were mounted in quartz capillaries of 0.1 mm diameter with mother liquid because of their propensity to lose crystallization solvents, while crystals **2** and **4** were cemented onto a quartz fiber with epoxy glue. Data were measured using ω scans of 0.3°/frame such that a hemisphere (1271 frames) was collected. No decay was indicated for any of four data sets by the recollection of the first 50 frames at the end of each data collection. The frames were integrated with the Bruker SAINT software package[49] using a narrow-frame integration algorithm, which also corrects for the Lorentz and polarization effects. Absorption corrections were applied using SADABS supplied by George Sheldrick.

The structures were solved and refined using the Bruker SHELXTL (version 5.1) software package,[50] in the space groups *C*2/*c*, *Pbcn*, $P\bar{1}$, and $P2_1/n$ for crystals **1**−**4**, respectively. Positions of all non-hydrogen atoms of diruthenium moieties were revealed by the direct method. In the case of crystals **1** and **2**, the asymmetric unit contains half of the molecule, which is related to the other half of the molecule by a crystallographic 2-fold axis orthogonal to the Ru1−Ru1A vector. One ethanol molecule was also located in the asymmetric unit of crystal **1**. The asymmetric unit of **3** contains three diruthenium molecules and one ethyl acetate molecules, while that of **4** contains one independent diruthenium molecule. With all non-hydrogen atoms being anisotropic and all hydrogen atoms in calculated positions and a riding mode, the structure was refined to convergence by the least-squares method on F^2, with SHELXL-93, incorporated in SHELXTL.PC V 5.03.

Acknowledgment. The generous support from both the University of Miami and the National Science Foundation (Grant CHE 0242623) is acknowledged.

Supporting Information Available: X-ray crystallographic files in CIF format for the structure determination of compounds **1**−**4**. This material is available free of charge via the Internet at http://pubs.acs.org.

IC035106K

(49) *SAINT V 6.035 Software for the CCD Detector System*; Bruker-AXS Inc.: Madison, WI, 1999.
(50) Sheldrick, G. M. *SHELXL-93, Program for the Refinement of Crystal Structures*; University of Göttingen: Göttingen, Germany, 1993.